Spectral linewidth of parallel Josephson junction array with intermediate-to-large damping

V. A. Shamporov,[1,2,3] A. S. Myasnikov,[2] E. V. Pankratova,[2] and A. L. Pankratov[1,2,3]
[1]*Institute for Physics of Microstructures of RAS, Nizhny Novgorod, Russia*
[2]*N.I. Lobachevsky State University of Nizhni Novgorod, Nizhny Novgorod, Russia*
[3]*Center of Cryogenic Nanoelectronics, Nizhny Novgorod State Technical University n.a. R.E. Alexeyev, Nizhny Novgorod, Russia*
(Received 26 May 2017; published 23 August 2017)

Spectral characteristics of THz generation in a parallel array of inductively coupled Josephson junctions with intermediate-to-large damping in the presence of thermal noise have been studied numerically. The influence of the number of junctions and coupling between them on the spectral linewidth has been investigated. We show that known theoretical formulas for radiation linewidth of a single Josephson junction, divided by the number of junctions in the chain, gives good agreement with numerical results for overdamped chains, while for chains with intermediate damping a factor of 1/2 has to be introduced into the formula in order to describe the linewidth on the I-V curve steps corresponding to lag-synchronization (soliton) regimes.

DOI: 10.1103/PhysRevB.96.064522

I. INTRODUCTION

One of the long-standing problems is the creation of THz-radiation generators that satisfy to a certain set of parameters, e.g., a long lifetime, compact size, low input voltage, and magnetic field demands, which are required for usage in gas component analysis on both industrial and academic scale. These requirements are crucial for various space missions (e.g., "Millimetron" [1]) due to payload weight and energy consumption restrictions. Josephson junctions could serve as a prospective basis of narrow linewidth as well as broadband generators (for example, flux-flow oscillators for use in noisy nonstationary spectrometers [2,3]) that correspond to such specifications. The Josephson junctions (JJs) are also used in digital electronics and quantum computing [4–9]. In the last years in long JJs various nontrivial fluctuational characteristics and effects, which can radically change the soliton propagations regimes, are studied, such as escape times [10–17], spectral linewidths [18–22], probabilities of spontaneous soliton formation due to Kibble-Zurek scenario [23], and noise suppression due to relativistic propagation of solitons [24,25]. However, the spectral characteristics of discrete Josephson arrays are weakly studied; mostly the processes of phase and lag synchronization (various soliton regimes) of JJ arrays [26–33] were investigated without account of noise.

Throughout this paper we will focus on one-dimensional parallel arrays (chains) of Josephson junctions and their spectral characteristics in the presence of thermal noise to find the parameter ranges suitable for construction of narrow-linewidth generators. Similar research has been performed, e.g., in Refs. [34,35] for overdamped chains and Refs. [18,21] for long underdamped Josephson junctions. We will be particularly interested in the chains with intermediate damping, which have been actually unexplored before numerically, although naturally appear for junctions based on shunted Nb junctions, as well as on high temperature superconductors, such as YBCO thin films [36–39]; see experimental results with such chains in Refs. [40,41]. Another important application of junctions with intermediate damping are JJ arrays that are used as basic elements and clock generators in rapid single flux quantum logic devices [4], however, in this case mostly thermal jitter rather than spectral characteristics has been studied [42–51]. Overdamped chains will also be taken into account in order to compare with the results of Refs. [34,35].

II. ANALYTICAL AND NUMERICAL MODELS

During our investigations we shall use the McCumber and Stewart's resistively and capacitively shunted junction (RCSJ) model for single JJ. According to this model, the time evolution of the wave function's phase difference φ across the junction (also known as the "Josephson phase") is governed by the following equation [52]:

$$\omega_p^{-2}\ddot{\varphi} + \omega_c^{-1}\dot{\varphi} + \sin\varphi = i + i_f(t), \tag{1}$$

where dots denote derivation with respect to t, ω_c is the characteristic frequency of the junction, ω_p is the junction plasma frequency, and i and i_f are the net current I flowing through the junction and the fluctuation current I_f, respectively, both normalized by the junction critical current I_c. Equation (1) can be written down in other forms through introduction of dimensionless time $\tilde{t}$:

$$\varphi'' + \alpha\varphi' + \sin\varphi = i + i_f(\tilde{t}) \quad \text{for } \tilde{t} = \omega_p t \tag{2a}$$

$$\beta\varphi'' + \varphi' + \sin\varphi = i + i_f(\tilde{t}) \quad \text{for } \tilde{t} = \omega_c t, \tag{2b}$$

where primes denote derivation with respect to $\tilde{t}$, $\alpha = \omega_p/\omega_c$ is the damping, and $\beta = \alpha^{-2}$. We will use the form (2a) throughout the rest of this paper.

The RCSJ model of a parallel chain of N inductively coupled Josephson junctions (see Fig. 1) represents the well-known Frenkel-Kontorova model [53,54] that has a broad variety of mechanical, chemical, biological, and physical applications including JJs-based digital circuits [4] and ballistic detectors [25,55]. To derive the corresponding equations one needs to consider the kth elementary cell composed by the kth and $k+1$th junctions. Applying Kirchhoff's laws to the cell yields the following equations:

$$V_k - V_{k+1} - L_k\dot{I}_{Lk} = 0, \quad I_{L,k-1} + I_{ek} = I_k + I_{Lk}, \tag{3}$$

where V_k is the voltage drop across the kth junction, I_k is the net current flowing through the kth junction, I_{ek} is the

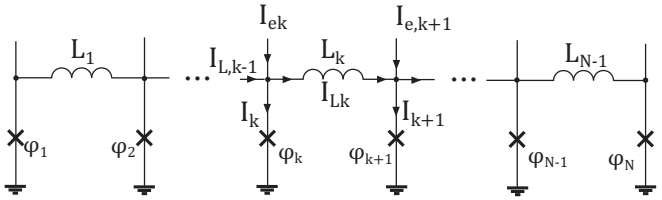

FIG. 1. A parallel chain of N inductively coupled Josephson junctions, with junctions shown as crosses.

respective external injection current, and I_{Lk} is the mesh (or loop) current through coupling inductor that gives rise to the self-induced magnetic field. The Josephson phase φ_k of the kth junction and the voltage V_k across it are related through the fundamental phase-voltage ratio:

$$\dot{\varphi}_k = \frac{2\pi}{\Phi_0} V_k, \tag{4}$$

where $\Phi_0 = \pi\hbar/e$ is the magnetic flux quantum. Substituting (4) into (3), we derive:

$$I_k = I_{ek} + \frac{\Phi_0}{2\pi}\left[\frac{\varphi_{k+1} - \varphi_k}{L_k} - \frac{\varphi_k - \varphi_{k-1}}{L_{k-1}}\right]. \tag{5}$$

In case of a uniform chain $L_k = L_0$, $I_{ek} = I$ for all $k = 1 \ldots N$; inserting I_k from (5) into (2a) gives:

$$\varphi_k'' + \alpha\varphi_k' + \sin\varphi_k = i + \frac{\varphi_{k+1} - 2\varphi_k + \varphi_{k-1}}{l} + i_{fk}(\tilde{t}), \tag{6}$$

where $i = I/I_c$—dimensionless injection current, $l = 2\pi I_c L_0/\Phi_0$—dimensionless inductance. This system of N differential equations (6) describes the chain of N parallel Josephson junctions with inductive coupling. We will only consider the situation with the reflective boundary conditions (i.e., when the side junctions are poorly matched and external magnetic field is absent), so the first and the last junctions in the chain are connected to only one neighbor [second and $(N-1)$th], respectively, so in the first and in the last equations only $(\varphi_2 - \varphi_1)/l$ and $(-\varphi_N + \varphi_{N-1})/l$ are present in the right hand side of Eq. (6), respectively.

We will study the radiation linewidth of this chain in the presence of thermal fluctuations (Gaussian white noise) i_{fk}: $\langle i_{fk}(\tilde{t}) i_{fn}(\tilde{t}+\tau)\rangle = 2\alpha\gamma\delta(\tau)\delta_{kn}$, uniform across all junctions. In the correlation function, α has arisen due to the introduction of dimensionless time $\tilde{t} = \omega_p t$, see (2a). Parameter γ defines the intensity of the noise and can be expressed as [52] $\gamma = (2e/\hbar)k_B T/I_c$, where $\hbar$ is the Planck's constant, e is the electron charge, k_B is Boltzmann's constant, and T is the temperature of the array. In the following, we will mostly consider the value of noise intensity $\gamma = 0.01$, roughly corresponding to 6–4 K temperature at typical technological parameters, except for the last figure where $\gamma = 0.002$ is taken to enlarge single soliton step. As we have checked, the linewidth decreases linearly with further decrease of noise. We have considered only thermal (natural) broadband noise, while technical (external interference) narrowband noises are neglected since in practice they can always be suppressed by proper grounding and filtering. It should be noted that in practice the dominating effect of technical noises can easily

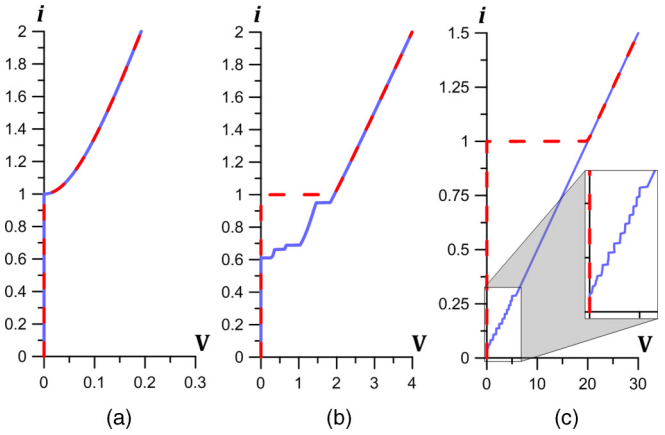

FIG. 2. Typical I-V curves of parallel JJ chains obtained in the RCSJ model (6) for varying damping parameters (a) $\alpha = 9.0$ (overdamped chain), (b) $\alpha = 0.5$ (intermediate damping), (c) $\alpha = 0.05$ (underdamped chain), $N = 15, l = 0.5, \gamma = 0$. Red dashed curves denote forward path of the I-V curve (increasing i from $i = 0$); blue solid curves denote return path of the I-V curve (decreasing i from $i > 1$).

be distinguished by measuring the spectra of the signal, since in this case the shape of spectral line will be Gaussian rather than Lorentzian for natural noises (see below).

The equation set (6) has been numerically integrated using both the Heun's method of integrating stochastic ODEs [56] and the implicit scheme (which is a straightforward generalization of a scheme listed in Ref. [57] with account of noise and was tested, e.g., in Refs. [10,11]), both demonstrating equivalent (in a statistical sense) results. Next, the power spectral density $S(\omega) = \langle \frac{1}{\tau} | \int_0^\tau v_k(\tilde{t}) e^{i\omega\tilde{t}}\, d\tilde{t}|^2 \rangle$ was computed [where $v_k(\tilde{t}) = \varphi'(\tilde{t})$ is a momentarily voltage at the kth junction and τ is the time span of the calculated numerical solution] and averaged over a certain ensemble of runs. Here, for a single junction only $v_1(\tilde{t})$ is considered, while for a junction chain the voltage for the first or the Nth junction is taken. After that, the frequency ω_0 and the linewidth $\Delta\omega$ of the main $S(\omega)$ peak were determined. To compute the spectral density, the standard fast Fourier transform method has been used with a number of time steps more than 2^{23} and rather long time span $\tau = 4 \times 10^5$ to resolve fine spectral structure. Here, the typical time step for implicit scheme was of order 0.05, while for Heun scheme of order 0.01. The mean dimensionless voltage V across the chain has been calculated as $V = \sum_{k=1}^{N} [\varphi_k(\tilde{t} + T_0) - \varphi_k(\tilde{t})]/NT_0$, where the time averaging period T_0 has been chosen to be much greater than the characteristic Josephson voltage oscillation period $2\pi/V$. Current-voltage (I-V) curves are defined as $i(V)$ (see Fig. 2 for an overview of I-V curves for various damping α). Lowering the parameter i from a value on the resistive branch of the I-V curve of the chain (i.e., $i > 1$) up to the superconductive branch ($i < 1$, depends on damping), we have computed the spectral linewidth $\Delta\omega$ (full width at half maximum) as a function of i.

An example of spectral density $S(\omega)$ for a single overdamped Josephson junction is presented in Fig. 3. One can see the main peak at the frequency $\omega_0 = \omega_J$ and higher harmonics

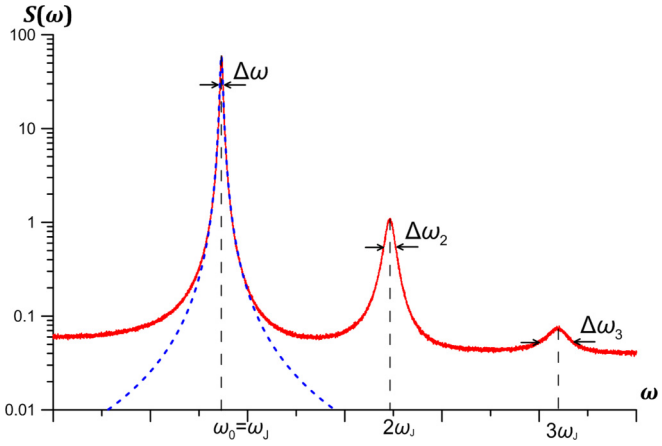

FIG. 3. Ensemble-averaged power spectral density $S(\omega)$ for a single overdamped Josephson junction ($\alpha = 10$, $i = 2.0$, $\gamma = 0.01$) with the main peak at fundamental Josephson frequency ω_J (equal to dimensionless junction voltage V) and harmonics at multiples of ω_J. Red curve—numerical results corresponding to model (2a), blue dashed curve—Lorentzian fit.

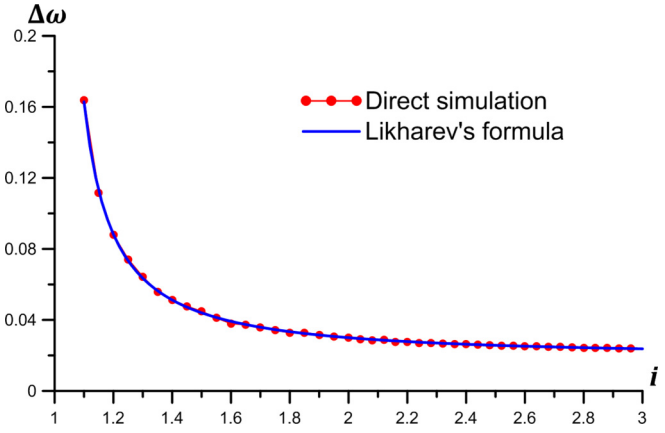

FIG. 4. Dependency of the spectral linewidth $\Delta\omega$ on bias current i for a single overdamped Josephson junction; $\gamma = 0.01$, $\alpha = 5.0$. Red curve with circles—numerical simulation of (2a), blue curve—formula (8).

at $2\omega_J$ and $3\omega_J$, respectively. We note that finite (nonzero) linewidth of harmonics appears due to diffusion of phase [58] and is proportional to the noise intensity. If the noise, leading to the phase diffusion, is narrowband (e.g., technical fluctuations and electromagnetic interference), then the shape of spectral line is Gaussian [58]. If, as in our case, the noise is broadband (thermal or shot fluctuations) then the form of the spectral line is Lorentzian [58] (see the dashed curve in Fig. 3). The analysis of the numerical results will be based upon existing theoretical formulas for a single junction. For a single JJ with arbitrary damping subjected to a broadband noise there exists an analytical expression [52,59] for the spectral linewidth $\Delta\omega$:

$$\Delta\omega = 2\alpha\gamma r_d^2, \tag{7}$$

where $r_d = dV/di$ is the differential resistance. In our numerical model, r_d was determined explicitly from I-V curves. A similar expression for $\Delta\omega$ may be found for overdamped junctions [52]:

$$\Delta\omega = 2\alpha\gamma r_d^2\left[1 + \frac{1}{2i^2}\right], \quad (\text{for } \alpha \gg 1) \tag{8}$$

which, through analytical derivation of $r_d = i/\alpha\sqrt{i^2 - 1}$ for overdamped junctions [52], may be transformed into the form:

$$\Delta\omega = \frac{2\gamma}{\alpha}\frac{i^2 + 0.5}{i^2 - 1}, \quad (\text{for } \alpha \gg 1). \tag{9}$$

The additional term in formula (8), as opposed to (7), explicitly describes the effect of parametric broadening of the linewidth [58]. This additional broadening occurs due to the interaction of second and higher-order JJ harmonics with the wideband thermal noise and subsequent down-conversion of these contributions to lower frequencies, where they add up with the main harmonic contribution. In Josephson junctions this effect naturally appears at bias current I just above the critical current I_c (i.e., where the magnitude of higher harmonics is high). Surprisingly, despite the approximate nature of Likharev's formula (8), it shows perfect agreement with the results of direct numerical simulations even for bias currents as small as $i = 1.1$ (Fig. 4) in the limit of small noise intensity γ.

It has been shown in Refs. [26,34] that parallel chains of N Josephson junctions exhibit a spectral linewidth $\Delta\omega$ (to not be confused with a resonance curve) around N times narrower than that of a single junction, which is due to stronger coupling between junctions, since a few adjacent elements behave as a single element due to mutual synchronization, that decreases the effect of noise. Thus, we have investigated the following fits for $\Delta\omega(i)$:

$$\Delta\omega = \frac{2\alpha\gamma r_d^2}{N}, \quad (\text{for } \alpha \lesssim 1) \tag{10}$$

$$\Delta\omega = \frac{2\alpha\gamma r_d^2}{N}\left[1 + \frac{1}{2i^2}\right], \quad (\text{for } \alpha \gg 1). \tag{11}$$

We have also studied the dependency of $\Delta\omega$ on l and N for values of $i \gtrsim 1.5$, i.e., at the parts of the I-V curves where $V(i)$ is linear (Fig. 2) and $\Delta\omega$ is almost constant, according to the following procedure. For each set with various l (or N, respectively) we have calculated $\Delta\omega(i,l,N)$ as usual for $i = 2.4$ to 2.5 and then averaged for this i range, which allowed us to find the desired $\Delta\omega(l,N)$. The differential resistance r_d has been averaged as well for comparison of $\Delta\omega(l,N)$ with (10).

III. RESULTS

A. Large damping ($\alpha \gg 1$)

Results of calculation for damping $\alpha = 3.0$ are presented in Figs. 5–7 as $\Delta\omega(i)$, $V(i)$, and $\omega_{peak}(i)$ graphs. One can see that the dependence of linewidth on bias current is in good agreement with both theoretical formulas (10), (11) in the most bias current range except vicinity of unity. Here the effect of parametric linewidth broadening (11) leads to better agreement with simulations for a larger number of junctions in the chain. The generation frequency in dimensionless units of ω_p at any point of the I-V curve is equal to the dimensionless voltage, as expected for the full-synchronization generation regime observed in overdamped chains.

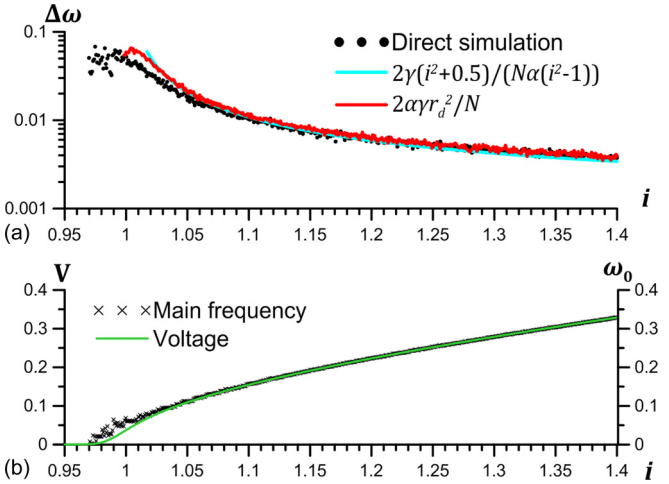

FIG. 5. (a) The linewidth vs bias current i and (b) the generation frequency and voltage for $N = 5$, $\gamma = 0.01$, $\alpha = 3.0$, $l = 0.5$.

To further check the validity of formula (10), we calculated the dependency $\Delta\omega(l)$ on the resistive branch of the I-V curve according to the procedure described in the previous section. The results are presented in Fig. 8. We have considered the most interesting practical range of dimensionless inductance, corresponding to the distance between JJs $\Delta x = \sqrt{l}$ from 0.3 to 100, where the length l is normalized to the Josephson length λ_J. For small values of the dimensionless inductance $l = 0.1$ to 1 the linewidth of the main peak is almost independent of l and corresponds to formula (10). With the increase of l the coupling between junctions in Eq. (6) decreases, and synchronization of oscillations along the chain degrades, which leads to the increase in $\Delta\omega$. Ultimately, for large chain inductances $l =$ 1000 to 10 000 the chain generation linewidth $\Delta\omega$ approaches the value for the single overdamped junction linewidth (9). However, significant reduction in linewidth of the chain in comparison to a single junction can still be observed at values of l as large as 50. Further, for larger values of l the linewidth of the chain is actually independent of N.

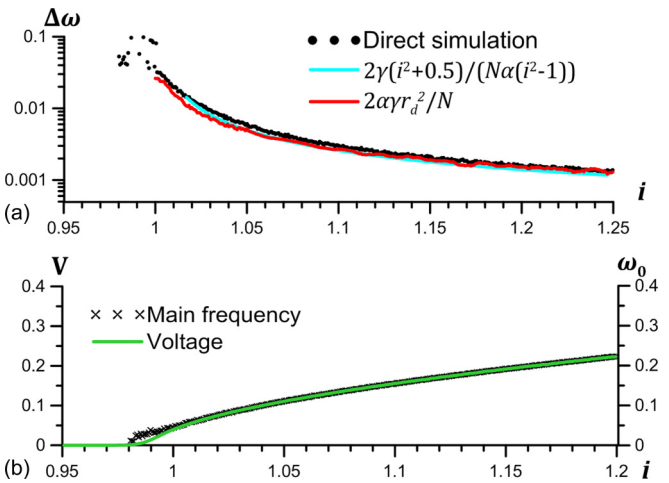

FIG. 6. (a) The linewidth vs bias current i and (b) the generation frequency and voltage for $N = 21$, $\gamma = 0.01$, $\alpha = 3.0$, $l = 0.5$.

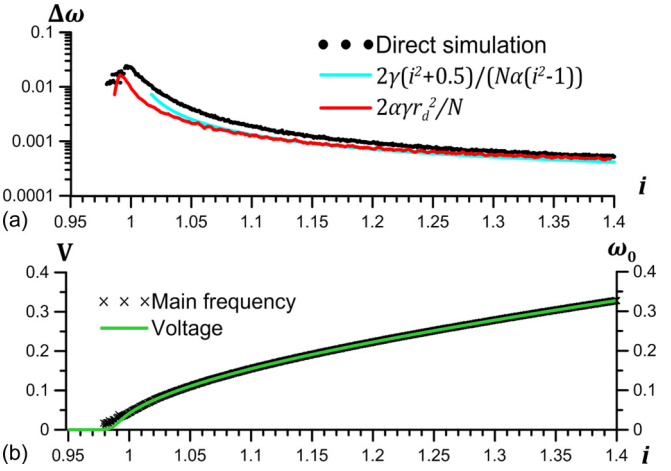

FIG. 7. (a) The linewidth vs bias current i and (b) the generation frequency and voltage for $N = 41$, $\gamma = 0.01$, $\alpha = 3.0$, $l = 0.5$.

In a slightly different perspective, Fig. 9 shows $\Delta\omega$ as a function of N for various values of dimensionless inductance l. For small l this dependency shows good agreement with (9), however, for large l the linewidth eventually stops decreasing with the increase of N. If one treats l as $l = \Delta x^2$—squared dimensionless distance between adjacent Josephson junctions in the chain with the total length $L = N\sqrt{l}$—then a conclusion may be made that there exists a certain critical length L_{cr} of synchronization among junctions. If L exceeds L_{cr}, then decrease of linewidth in the chain does not occur. This result has also been obtained in Ref. [60], however, the damping parameter value α for that result was not specified and the function $\Delta\omega(N)$ approaches constant at much lower values of l than in our calculations. Comparing results for $\alpha = 3.0$ and $\alpha = 9.0$ in Fig. 9, one can see that L_{cr} does not depend strongly on α in the overdamped limit $\alpha \gg 1$.

B. Intermediate damping ($\alpha \lesssim 1$)

For damping $\alpha < 1$ current-voltage characteristic of a parallel chain exhibits sharp steps at return-path I-V curve

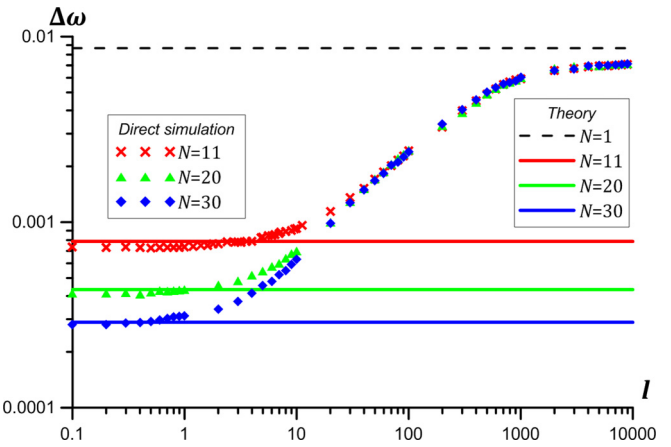

FIG. 8. Spectral linewidth as a function of inductance l at $i \approx 2.45$ for $\gamma = 0.01$, $\alpha = 3.0$, and various N. Symbols denote results of direct linewidth calculation, solid lines denote theoretical dependency (10), and the dashed line denotes dependency (9) for $i = 2.45$.

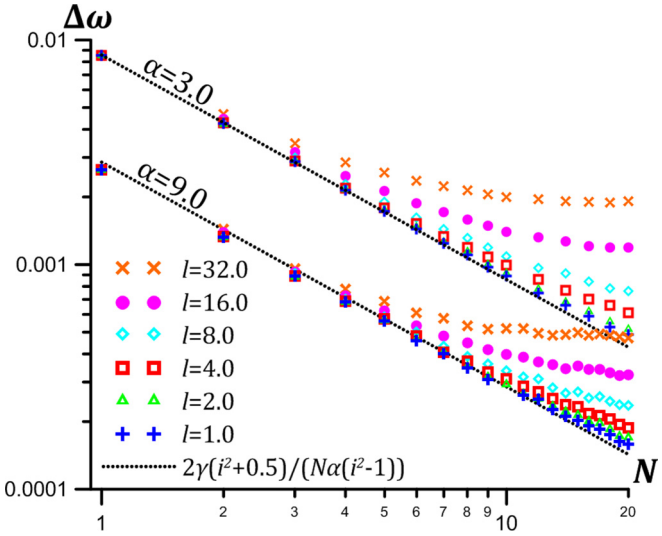

FIG. 9. Spectral linewidth as a function of number of junctions in chain N at $i \approx 2.45$ for $\gamma = 0.01$ and varying inductance l. Symbols denote results of direct linewidth calculation, dotted line denotes theoretical dependency (9) for $i = 2.45$; two sets of results are presented, for $\alpha = 3.0$ and $\alpha = 9.0$.

for bias currents $i < 1$ [see Fig. 2(b)]. These steps correspond to a lag-synchronization regime with an integer number of voltage solitons traveling along the chain, as opposed to the phase synchronization regime on the resistive branch of the I-V curve for $i > 1$ [Fig. 10(b)], where all junctions of the chain oscillate in-phase with each other. The generalization of linewidth analysis for such chains is complicated by the strong dependency of the total number of current-wise location of steps on N even in the absence of noise. For example, in Fig. 10(a) I-V curves for $N = 21$ and $N = 22$ change

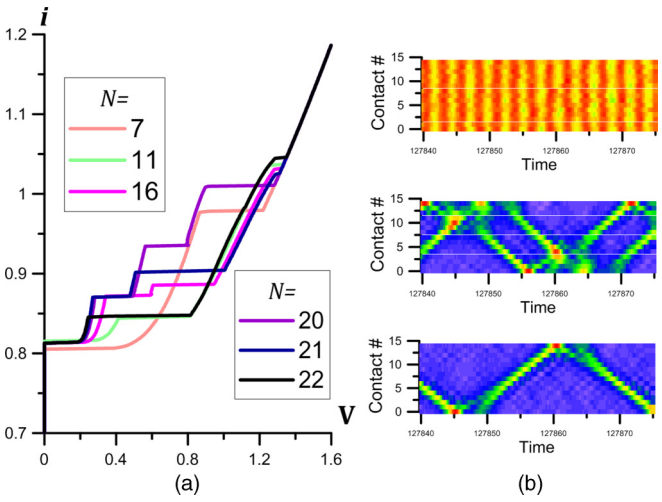

FIG. 10. (a) I-V curves for $\gamma = 0$, $\alpha = 0.5$, $l = 0.7$. (b) Voltage dynamics along the chain with $\gamma = 0.01$, $\alpha = 0.5$, $l = 0.5$, $N = 15$. Top to bottom: $i = 1.19$ (resistive I-V curve branch), $i = 0.7$ (second return-path step), $i = 0.65$ (first return-path step); junction numbers are shown at the y axis, simulation time is shown at the x axis, voltage magnitude is shown by its hue; warmer colors—higher voltage, colder colors—lower voltage.

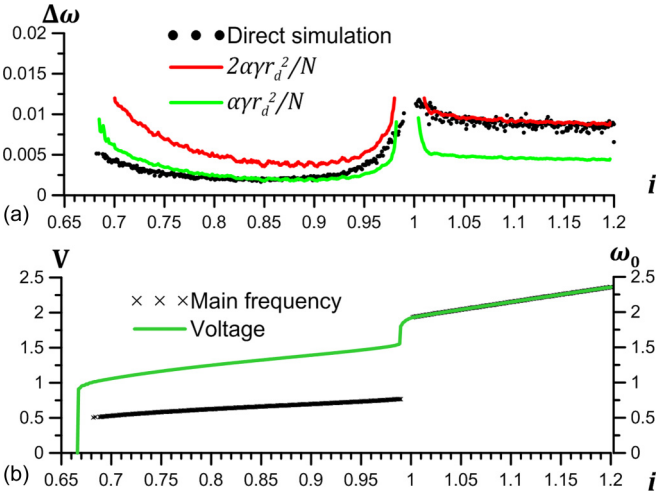

FIG. 11. (a) The linewidth vs bias current i and (b) the generation frequency and voltage for $N = 5$, $\gamma = 0.01$, $\alpha = 0.5$, $l = 0.5$ for IV curve with one sharp step.

significantly, although the chains differ by one junction only. We will therefore consider the model cases of chains with one and two steps: The results are presented in Figs. 11–14.

For the resistive branch of the I-V curve of Josephson junction chains with intermediate damping the linewidth of the main spectral peak is in good agreement with formula (10); the fundamental frequency ω_0 is equal to voltage V in dimensionless units. At the steps of I-V curves, however, the modified Josephson voltage-to-frequency relation holds, and ω_0 is equal to $V/2$. The nontrivial observation is that the spectral linewidth in this case, in fact, is better described by the formula

$$\Delta\omega = \frac{\alpha\gamma r_d^2}{N} \tag{12}$$

than by formula (10), so the linewidth is halved in proportion to the halved frequency. This is observed for chains with any number of steps, e.g., with 1 step (Fig. 11) and 2 steps (Fig. 12)

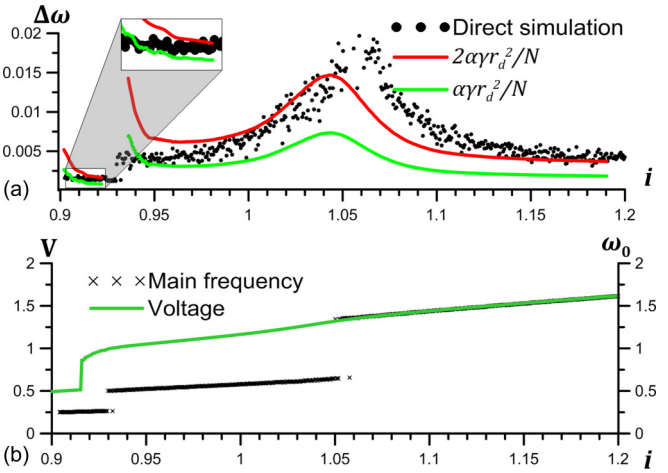

FIG. 12. (a) The linewidth vs bias current i and (b) the generation frequency and voltage $N = 11$, $\gamma = 0.01$, $\alpha = 0.7$, $l = 0.5$ for IV curve with one sharp and one smooth step.

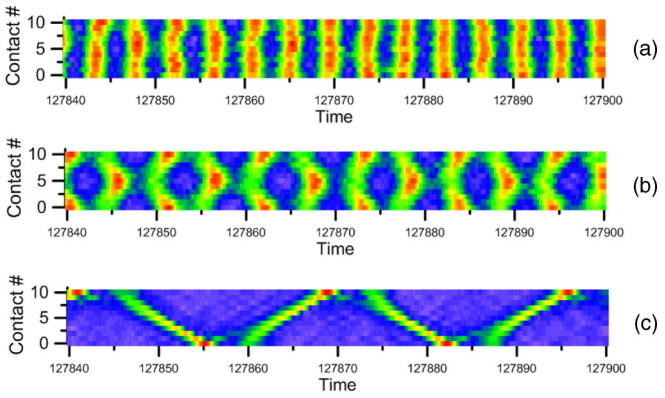

FIG. 13. Voltage dynamics for chain with $N = 11$, $\gamma = 0.002$, $\alpha = 0.7$, $l = 0.5$, see I-V curve in Fig. 12 at bias currents: (a) $i = 1.105$ (resistive I-V curve branch), (b) $i = 1.0$ ("smooth" step), (c) $i = 0.925$ (conventional "sharp" step); junction numbers are shown at the y axis, simulation time is shown at the x axis, voltage magnitude at the point is shown by its hue; warmer (lighter) colors—higher voltage, colder (darker) colors—lower voltage.

at their respective I-V curves and is different by an additional factor of 1/2 with the result for strongly underdamped case of a shuttle fluxon oscillator [18]. Similar linewidth halving has been recently shown for underdamped systems [61], but the regime of one traveling soliton [18] has not been studied due to a huge amount of required simulation time. Here we partly resolve this problem by transition to damping of order unity, which makes the problem numerically tractable and confirms the linewidth halving (12) for a single soliton regime, but we are still in the discrete case of a limited number of junctions in the chain, which is far from the continuous limit of Ref. [18].

Another peculiar feature is the appearance of the "smooth" steps at I-V curves of chains with intermediate damping. In Fig. 12, the step adjacent to the resistive I-V branch does not exhibit a sudden voltage jump and corresponding change in linewidth at values of bias current i close to unity (critical current value); instead, both voltage and linewidth change gradually, with the linewidth reaching a maximum value in the "transition" current region from smooth step to ohmic line and minimum in the middle of the smooth step. The generation

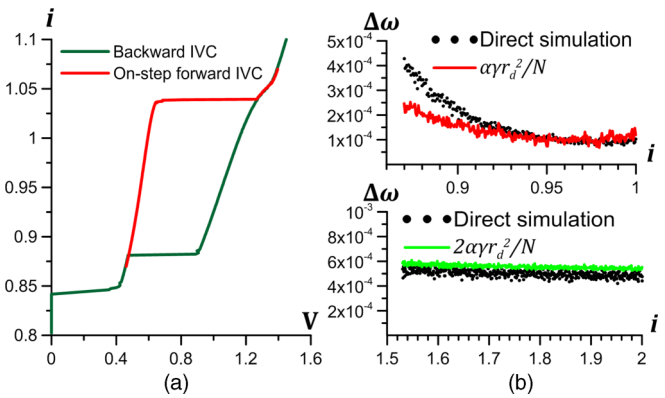

FIG. 14. (a) I-V curves showing hysteretic behavior at the steps; (b) linewidths $\Delta\omega$ at the resistive branch of I-V curve (bottom) and at the sharp step (top) for $N = 11$, $\gamma = 0.002$, $\alpha = 0.7$, $l = 0.5$.

frequency ω_0 switches its value from V to $V/2$ at i slightly larger than unity and persists at $V/2$ throughout all of the "smooth" step length. At the low-current end of this "smooth" step, the linewidth approaches the value predicted by (12). At even lower currents a conventional I-V step corresponding to one traveling soliton is observed, where $\Delta\omega$ is again better described by (12) than (10).

One possible explanation of this "smooth" step phenomenon may be derived from comparing the chain voltage dynamics at the smooth transition I-V curve region [Fig. 13(b)] and at the resistive I-V curve branch [Fig. 13(a)]. The step adjacent to the resistive I-V curve branch contains the maximum possible number of solitons (which is two in this case). In a chain with large L the two solitons would have followed each other in a compact train [see, for example, Fig. 10(b), middle graph]; however, in the case of Fig. 13 due to the restricted dimensionless length of the chain and reflection from chain ends these two solitons move in opposite directions, thus forming a "standing wave" [Fig. 13(b)], representing itself as a cluster synchronization. This regime of cluster synchronization is qualitatively close to the phase synchronization regime observed at the resistive I-V branch [Fig. 13(a)] and so a smooth transition from phase synchronization to two-soliton synchronization comes as natural. On the other hand, the next step at the I-V curve contains only one soliton [Fig. 13(c)], which is unable to form a standing wave by itself; the single-soliton regime is qualitatively different from the standing wave regime and so a sharp step at the I-V curve is observed.

Conventional I-V curve steps in Josephson chains with $\alpha < 1$ are highly hysteretic, which is not the case with the "smooth" step at Fig. 12. The single soliton step at I-V curve of Fig. 12 is still hysteretic; increasing i after initially biasing it at the sharp step allows it to stay at the same step for much larger values of i than was possible on the return path [Fig. 14(a)]. For this elongated step the spectral linewidth [at $\omega_0 = V/2$, Fig. 14(b)] is also in good agreement with formula (12), which further proves the validity of this new relation on I-V curve steps of Josephson chains.

IV. CONCLUSIONS

Spectral characteristics of generation in a parallel array of Josephson junctions have been numerically studied within the frame of Frenkel-Kontorova model with noise. The comparison of Likharev's formula for a single junction linewidth (8) with computer simulation results demonstrates perfect agreement in the low noise limit. We have also shown good agreement of numerical and theoretical results for generation linewidth of parallel overdamped ($\alpha \gg 1$) JJ chains, as long as the coupling between junctions is sufficiently strong (i.e., the dimensionless inductance l is small). Here the theoretical formula (11) represents a single junction linewidth (8), divided by a number of junctions N. For weak coupling the linewidth effectively stops decreasing with the increase of number of junctions in the chain, which indicates the limiting number of junctions in parallel arrays of Josephson oscillators and logic devices. In particular, for typical inductances of order 0.5–1 the chains of 20–30 junctions can be recommended to keep the minimal linewidth. For parallel chains of Josephson

junctions with intermediate damping ($\alpha \lesssim 1$) the linewidth at the steps of current-voltage characteristics (corresponding to lag-synchronization/soliton regimes) is better described by formula (12), so an additional factor of 1/2 appears in comparison with overdamped junctions due to modified Josephson relation. Also, under special conditions (sufficiently small dimensionless chain length $L = N\sqrt{l}$, where N is the number of junctions in the chain), a "smooth" step at the I-V curve of arrays with intermediate damping may be observed, if the voltage solitons emerging at the step form a standing wave/cluster synchronization, where the same linewidth formula (12) is valid. Due to a drastic decrease in differential resistance at I-V curve steps (with lag-synchronization oscillation regime) when compared to the resistive I-V curve branch (phase synchronization regime) the linewidth of generation is, respectively, decreased, which makes the I-V curve steps a prospective operating point for THz generators based on Josephson junction arrays even for junctions with intermediate damping $\alpha \lesssim 1$.

ACKNOWLEDGMENTS

This work is supported by Russian Science Foundation (Project 16-19-10478). The main part of the results has been calculated using the "Lobachevsky" supercomputing cluster of NNSU.

[1] http://millimetron.asc.rssi.ru/index.php/en/
[2] V. L. Vaks, V. V. Khodos, and E. V. Spivak, Rev. Sci. Instrum. **70**, 3447 (1999).
[3] E. A. Matrozova, A. L. Pankratov, and L. S. Revin, J. Appl. Phys. **112**, 053905 (2012).
[4] K. K. Likharev and V. K. Semenov, IEEE Trans. Appl. Supercond. **1**, 3 (1991); P. Bunyk, K. Likharev, and D. Zinoviev, Int. J. High Speed Electron. Syst. **11**, 257 (2001).
[5] Yu. Makhlin, G. Schön, and A. Shnirman, Rev. Mod. Phys. **73**, 357 (2001).
[6] D. V. Averin, K. Rabenstein, and V. K. Semenov, Phys. Rev. B **73**, 094504 (2006).
[7] T. Ohki, A. Savin, J. Hassel, L. Gronberg, T. Karminskaya, and A. Kidiyarova-Shevchenko, IEEE Trans. Appl. Supercond. **17**, 128 (2007).
[8] A. Fedorov, A. Shnirman, G. Schön, and A. Kidiyarova-Shevchenko, Phys. Rev. B **75**, 224504 (2007).
[9] A. Herr, A. Fedorov, A. Shnirman, E. Ilichev, and G. Schön, Supercond. Sci. Technol. **20**, S450 (2007).
[10] K. G. Fedorov and A. L. Pankratov, Phys. Rev. B **76**, 024504 (2007).
[11] K. G. Fedorov and A. L. Pankratov, Phys. Rev. Lett. **103**, 260601 (2009).
[12] G. Augello, D. Valenti, A. L. Pankratov, and B. Spagnolo, Eur. Phys. J. B **70**, 145 (2009).
[13] D. Valenti, C. Guarcello, and B. Spagnolo, Phys. Rev. B **89**, 214510 (2014).
[14] C. Guarcello, D. Valenti, A. Carollo, and B. Spagnolo, Entropy **17**, 2862 (2015).
[15] C. Guarcello, D. Valenti, and B. Spagnolo, Phys. Rev. B **92**, 174519 (2015).
[16] C. Guarcello, D. Valenti, A. Carollo, and B. Spagnolo, J. Stat. Mech.: Theory Exp. (2016) 054012.
[17] C. Guarcello, D. Valenti, B. Spagnolo, V. Pierro, and G. Filatrella, Nanotechnology **28**, 134001 (2017).
[18] E. Joergensen, V. P. Koshelets, R. Monaco, J. Mygind, M. R. Samuelsen, and M. Salerno, Phys. Rev. Lett. **49**, 1093 (1982).
[19] A. L. Pankratov, Phys. Rev. B **65**, 054504 (2002).
[20] V. P. Koshelets, P. N. Dmitriev, A. S. Sobolev, A. L. Pankratov, V. V. Khodos, V. L. Vaks, A. M. Baryshev, P. R. Wesselius, and J. Mygind, Physica C (Amsterdam) **372-376**, 316 (2002).
[21] A. L. Pankratov, Appl. Phys. Lett. **92**, 082504 (2008).
[22] A. L. Pankratov, Phys. Rev. B **78**, 024515 (2008).
[23] A. V. Gordeeva and A. L. Pankratov, Phys. Rev. B **81**, 212504 (2010).
[24] A. L. Pankratov, A. V. Gordeeva, and L. S. Kuzmin, Phys. Rev. Lett. **109**, 087003 (2012).
[25] I. I. Soloviev, N. V. Klenov, A. L. Pankratov, E. Ilichev, and L. S. Kuzmin, Phys. Rev. E **87**, 060901(R) (2013).
[26] A. K. Jain, K. K. Likharev, J. E. Lukens, and J. E. Sauvageau, Phys. Rep. **109**, 309 (1984).
[27] S. G. Lachenmann, G. Filatrella, A. V. Ustinov, T. Doderer, N. Kirchmann, D. Quenter, R. P. Huebener, J. Niemeyer, and R. Pöpel, J. Appl. Phys. **77**, 2598 (1995).
[28] P. A. A. Booi and S. P. Benz, Appl. Phys. Lett. **68**, 3799 (1996).
[29] A. V. Ustinov, B. A. Malomed, and S. Sakai, Phys. Rev. B **57**, 11691 (1998).
[30] P. Barbara, A. B. Cawthorne, S. V. Shitov, and C. J. Lobb, Phys. Rev. Lett. **82**, 1963 (1999).
[31] D. Abraimov, P. Caputo, G. Filatrella, M. V. Fistul, G. Yu. Logvenov, and A. V. Ustinov, Phys. Rev. Lett. **83**, 5354 (1999).
[32] G. Filatrella, N. F. Pedersen, and K. Wiesenfeld, Phys. Rev. E **61**, 2513 (2000); IEEE Trans. Appl. Supercond. **11**, 1184 (2001).
[33] G. Filatrella, B. Straughn, and P. Barbara, J. Appl. Phys. **90**, 5675 (2001).
[34] V. K. Kornev, I. I. Soloviev, J. Oppenlaender, Ch. Haeussler, and N. Schopoh, Supercond. Sci. Technol. **17**, S406 (2004).
[35] V. K. Kornev, I. I. Soloviev, N. V. Klenov, T. V. Filippov, H. Engseth, and O. A. Mukhanov, IEEE Trans. Appl. Supercond. **19**, 916 (2009).
[36] D. Winkler, Y. M. Zhang, P. A. Nilsson, E. A. Stepantsov, and T. Claeson, Phys. Rev. Lett. **72**, 1260 (1994).
[37] Y. M. Zhang, D. Winkler, P.-A. Nilsson, and T. Claeson, Phys. Rev. B **51**, 8684 (1995).
[38] D. Terpstra, R. P. J. IJsselsteijn, and H. Rogalla, Appl. Phys. Lett. **66**, 2286 (1995).
[39] L. S. Revin, A. V. Chiginev, A. L. Pankratov, D. V. Masterov, A. E. Parafin, G. A. Luchinin, E. A. Matrozova, and L. S. Kuzmin, J. Appl. Phys. **114**, 243903 (2013).
[40] G. Kunkel, R. H. Ono, and A. M. Klushin, Supercond. Sci. Technol. **9**, A1 (1996).
[41] K. Lee, I. Iguchi, J. Kim, S.-K. Han, and K.-Y. Kang, IEEE Trans. Appl. Supercond. **7**, 3399 (1997).

[42] A. V. Rylyakov and K. K. Likharev, IEEE Trans. Appl. Supercond. **9**, 3539 (1999).
[43] H. Terai, Z. Wang, Y. Hishimoto, S. Yorozu, A. Fujimaki, and N. Yoshikawa, Appl. Phys. Lett. **84**, 2133 (2004).
[44] A. L. Pankratov and B. Spagnolo, Phys. Rev. Lett. **93**, 177001 (2004).
[45] H. Terai, Y. Hashimoto, S. Yorozu, A. Fujimaki, N. Yoshikawa, and Z. Wang, IEEE Trans. Appl. Supercond. **15**, 364 (2005).
[46] T. Ortlepp and F. Hermann Uhlmann, IEEE Trans. Appl. Supercond. **15**, 344 (2005).
[47] V. K. Semenov and A. Inamdar, IEEE Trans. Appl. Supercond. **15**, 435 (2005).
[48] Q. P. Herr, D. L. Miller, and J. X. Przybysz, Supercond. Sci. Technol. **19**, S387 (2006).
[49] A. V. Gordeeva and A. L. Pankratov, Appl. Phys. Lett. **88**, 022505 (2006).
[50] T. Ortlepp and F. Hermann Uhlmann, IEEE Trans. Appl. Supercond. **17**, 534 (2007).
[51] A. V. Gordeeva and A. L. Pankratov, J. Appl. Phys. **103**, 103913 (2008).
[52] K. K. Likharev, *Dynamics of Josephson Junctions and Circuits* (Gordon and Breach, New York, 1986), p. 634.
[53] Y. S. Kivshar and B. A. Malomed, Rev. Mod. Phys. **61**, 763 (1989).
[54] O. M. Braun and Yu. S. Kivshar, *The Frenkel-Kontorova Model: Concepts, Methods, and Applications* (Springer-Verlag, Berlin, 2004).
[55] V. K. Semenov and D. V. Averin, IEEE Trans. Appl. Supercond. **13**, 960 (2003).
[56] R. Mannella, Int. J. Mod. Phys. C **13**, 1177 (2002).
[57] P. S. Lomdahl, O. H. Soerensen, and P. L. Christiansen, Phys. Rev. B **25**, 5737 (1982).
[58] A. N. Malakhov, *Fluctuations in Autooscillating Systems* (Science, Moscow, 1968) (in Russian).
[59] A. J. Dahm, A. Denestein, D. N. Langenberg, W. H. Parker, D. Rogovin, and D. J. Scalapino, Phys. Rev. Lett. **22**, 1416 (1969).
[60] V. K. Kornev and A. V. Arzumanov, Tech. Phys. Lett. **26**, 102 (2000).
[61] A. L. Pankratov, E. V. Pankratova, V. A. Shamporov, and S. V. Shitov, Appl. Phys. Lett. **110**, 112601 (2017).